Pulsed, Millinewton Class Metal Plasma Thruster for Broad Mission Applications

Small Sat Europe 2025

Mahadevan Krishnan[a]
AASC, Oakland, CA, 94611, USA

John Kent Frankovich[b]
Benchmark Space Systems, Burlington, VT, 05401, USA

ABSTRACT: The Metal Plasma Thruster (MPT) operates with any metal propellant (Mg: ISP 2022s, Mo: ISP 1774s, Al: ISP 1575s, Cu: ISP 1348s, etc.). The MPT directly converts cold metal into a hot plasma burst that is ejected into a narrow cone with an axial speed of 17.4 km/s (Mo). The thruster requires no gases, liquids, valves or flow controls. The MPT is modular, with a Unit Cell volume 96 mm x 96 mm x 68 mm (0.63 L) and mass of 1.4 kg. The Pulsed thruster delivers a fixed thrust/power of 10 μN/W, over a wide range of input power, with the upper limit set by thermal management of waste heat. The typical unit cell (4 metal pucks of ≈130 g each) operates at up to 100W (1 mN thrust at 5 Hz rep-rate). The impulse bit/pulse is 0.2 mNs. With multiple firings the thruster gives an impulse of 11 Ns/g of propellant. With 520g of propellant loaded, the potential total impulse is ≈5700 Ns from the unit cell. Life tests in vacuum continue towards this goal. The PPU is rad-tolerant, accepts a wide range of DC input and operates at 45V DC. The MPT, unlike its peers the In FEEPs or Iodine ion engines, requires no standby heater, electron neutralizer or multi-kV DC potentials. The environmentally qualified MPT has been launched into LEO in Jan. 2023 and again in Mar. 2024 and awaits a third launch scheduled for Aug. 2025. The MPT thruster has been fired in vacuum for >15,000 hours of operation. Multiple tests on a pendulum thrust stand at NASA/GRC have measured thrust and impulse bits (published) for many metals.

[a] President, Alameda Applied Sciences, krish@aasc.space.
[b] VP, Electric Propulsion, kfrankovich@benchmark-space.com.

I. Introduction

This paper describes a pulsed Metal Plasma Thruster (MPT) that provides ~1 mN drag compensation for micro- and mini-satellites (10 kg – 180 kg mass) in VLEO, while also serving as a complement to Chemical Propulsion or Hall Effect Thrusters for larger satellites in LEO and beyond.

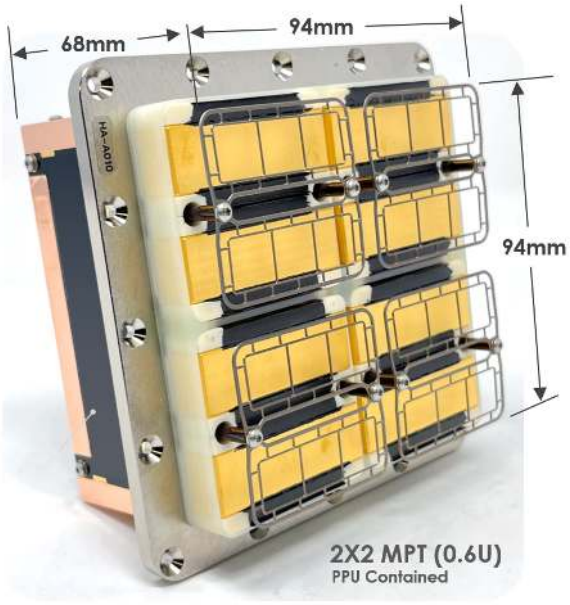


Figure 1: Xantus MPT

Figure 1 shows the Xantus MPT, presently manufactured under license by Benchmark Space Systems.

The MPT delivers thrust/impulse by eroding tiny amounts of the fuel metal (Mo in this case) and ejecting that Mo as a fast, hot (~3 eV) plasma "supersonic" jet into vacuum.

Figure 2 shows a simplified diagram of its operation. The PPU delivers a short current pulse to the Mo fuel puck that ejects a fast plasma "blob" to give an impulse bit. The PPU is charged to 45 V. It discharges about 0.6 C in ~5ms into a cathodic discharge between the puck and a highly transparent anode grid located about 10-mm above it. This arc discharge erodes ≈1.8x10^{-8} kg of Mo as plasma and ejects it into a narrow (supersonic) cone at a speed of 17.4 km/s. This gives an (ideal) individual impulse bit on each shot of ≈340 μNs. This ideal impulse bit must be corrected for anode transmission loss (about 15%), imperfect ionization (plasma is only 95% ionized) and plume divergence loss (≈20%). The net correction is: 85%*95%*80% = 65%. The useful impulse bit/shot is ≈220 μNs. If this is repeated at say, 5 Hz, the average thrust would be ≈1.1 mN. The average power into the PPU at 5 Hz is ≈110 W. The Thrust/Power ratio of the MPT is ≈10 μN/W. This T/P ratio is constant and independent of input power! The MPT operates stably over a wide range of power with constant T/P provided that the heat dissipation (≈70% of input power) is managed by the satellite.

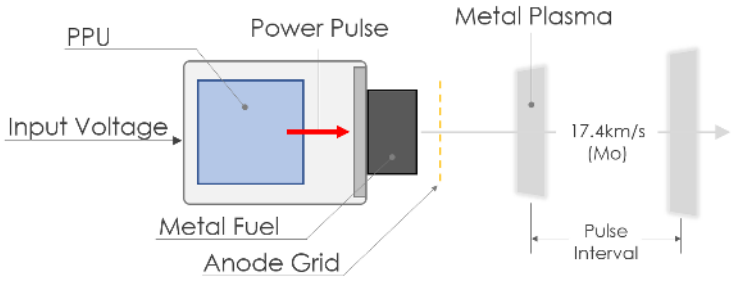


Figure 2: Impulse bit of the MPT from ejected metal plasma

This paper is organized as follows: **section II** describes the structure and operation of the MPT. The descriptions are brief as these have been described in detail in earlier publications [Refs. 1, 2]. **Section III** presents a summary of in-house vacuum testing and impulse bit and thrust measurement campaigns conducted at NASA GRC. Three campaigns tested an MPT consisting of four identical, square "pucks" of Molybdenum (Figure 1). Another campaign tested a Xantus thruster with three different pucks: Molybdenum, Copper and Stainless Steel. The Mo and Cu pucks were made of solid metal (identical in shape to the four pucks in Figure 1), but the stainless-steel puck was comprised of a sandwich of thin sheets of stainless steel identical to the steel used in the balloon tanks of launch vehicle upper stages that have been discarded in orbit and pose a potential collision hazard to the increasing number of smaller satellites that now occupy LEO. Small satellite numbers are growing rapidly. It will become critically important to remove the large, useless rocket bodies in LEO before one of them collides with other satellites and, in the worst case, provokes the Kessler syndrome. **Section IV** presents a comparative study of the MPT and its peers in the mN thrust class, such

as the Indium FEEP [Ref. 3], the Iodine ion engine [Ref. 4] and lower power Hall Thrusters [Ref. 5]. **Section V** is a summary, followed by acknowledgments and references.

II. MPT OPERATION

A. METAL PLASMA THRUSTER OPERATION

The MPT uses a low voltage capacitor and solid metal propellant to eject plasma at high speed to produce thrust. The MPT offers variable ISP (693 s to 3119 s) by using different metal propellants.

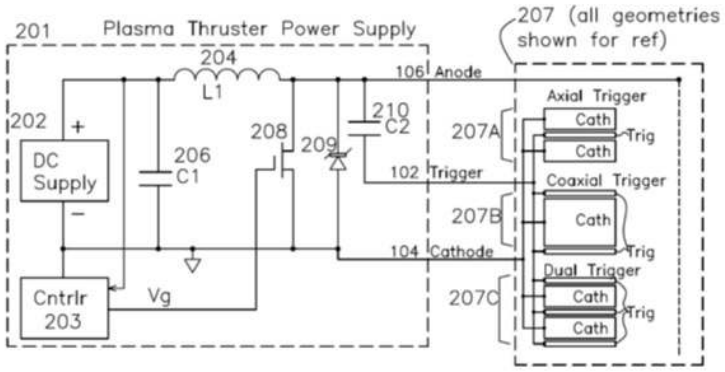


Figure 3: Electrical equivalent circuit of the PPU

Figure 3 is an electrical equivalent circuit of the PPU. A typical operating sequence is as follows: the controller switches on the DC Supply (202) to charge the capacitor C1 (206) to a set voltage, typically 45 V. When the capacitor voltage reaches the set point, the controller gates the MOSFET switch (208) into conduction by sending a gate pulse. The capacitor drives a current through the inductor L1 (204) and the switch. This current rises to 150 A in ≈60 µs. At this point, the switch is opened, by turning off the gate pulse. The switch opens in ~100 ns and coil L1 generates an LdI/dt voltage spike of up to 1 kV that appears at blocking capacitor C2 (210) and at the anode (106). Capacitor C2 (210) and the thin film resistance across the trigger path act as a high pass filter, passing the fast-rising voltage pulse to the thin film, in which are created several micro-discharges that emit plasma that expands to fill the vacuum gap between the cathode and the anode screen. This surface flashover (trigger) plasma expands at a typical speed of 1 cm/µs and crosses the 9 mm vacuum gap in approximately 1 µs. The plasma fills the vacuum gap on a time scale of a few times this transit time, or a few µs. This plasma bridge allows current flow from the cathode across to the W anode. The trigger current path is cutoff, both because the resistance is much higher than the arc discharge resistance of 50 mΩ and because the high pass filter formed by C2 and the thin film becomes a high impedance path on the slower time scale (~3 ms) of the arc discharge. When the voltage across the arc discharge drops below the sheath voltage (18 V – 25 V), the current is cutoff. This operational sequence of events is described with measured data in the next section.

Trigger Phase operation

Figure 4 shows measured and computed current and voltage during the trigger phase of the MPT pulse. The graph shows five traces. The dashed green trace is the ignition coil current calculated before the switch is opened, using C1, V=45 V, L1 and a total loop resistance of 50 mΩ (of C1, L1, MOSFETs in parallel and connections). At the start of each pulse, the MOSFETS are gated closed and current flows from C1 and L1 through the MOSFETS back to ground. At ≈60 µs and a current of 150 A, the MOSFETs are gated open. The yellow trace is the measured capacitor voltage that starts at 45 V and drops to about 43 V at the arc switch time. The green solid line is the capacitor voltage calculated by numerically integrating the circuit equations, assuming an arc sheath drop of 24 V and an arc resistance of 44 mΩ. The arc current is the blue trace, measured from target to anode, and is barely distinguishable from the red calculated current. This arc

current flows after a slight dip during the opening phase of a few microseconds. There is good agreement between model and data. The charge lost to the MOSFETs during a typical shot is <3% of the total charge driven into the arc plasma, making the driver circuit highly energy efficient.

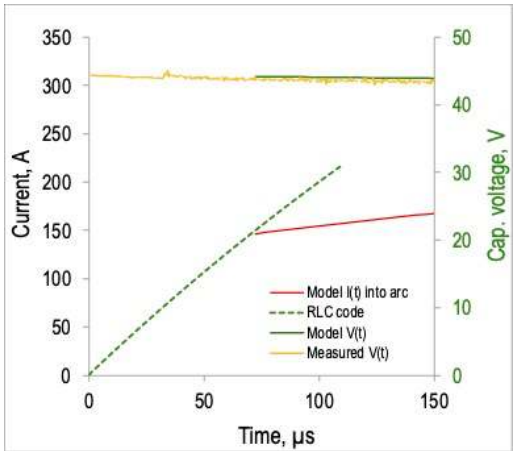


Figure 4: Trigger phase of MPT pulse

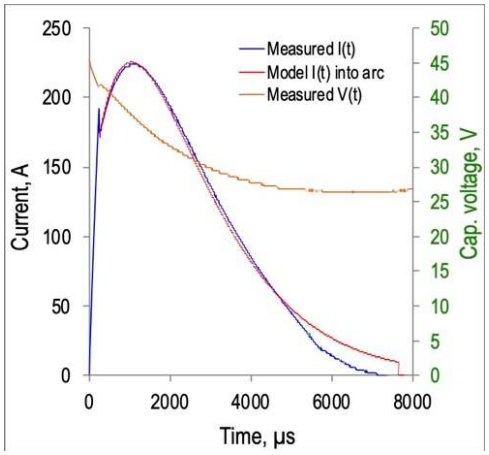


Figure 5: Arc discharge phase of MPT pulse

Arc Discharge Phase operation

Figure 5 shows the measured arc current (blue line) and the current computed by integrating the circuit equation (red line). The computed current assumed a sheath drop of 24 V and a plasma resistance of 44 mΩ. The measured and computed voltages on the capacitor (brown dashed and solid green lines) are the same as in Figure 4, but shown on an extended time scale. The assumed arc resistance of 30 mΩ is consistent with a Spitzer resistance of a plasma column that is ≈1.2 cm in diameter, 0.9 cm long, with an electron temperature of 3 eV and a mean ion charge of 2. These values are based on measured quantities in cathodic arcs by several [6] authors. The MPT performance during the trigger and arc phases has been benchmarked against a theoretical model. The agreement between the model and measured current and voltage provides us with a useful predictive tool to optimize future designs.

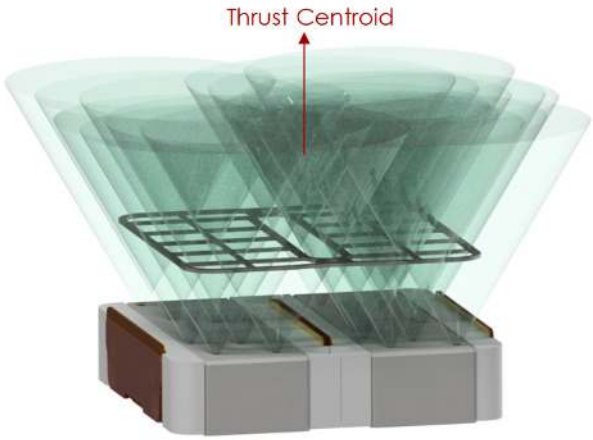


Figure 6: **Multiple spots create Mo plasma in a cone of expansion from the puck surface**

The MPT uses pulsed cathodic arcs to generate very tiny impulse bits. By firing the thruster repetitively (at rates of 1Hz – 10Hz), these impulse bits cumulatively provide useful impulse to affect the orientation or orbital radius of satellites in a broad mass range from CubeSats to ESPA Class satellites in VLEO, LEO, MEO and GEO. The cathodic arc discharge of the MPT erodes and ionizes the metal propellant from tiny spots (~1 µm in size) on the puck surface into a plasma cone that expands into the vacuum at speeds of 6.8 km/s – 30.6 km/s, depending upon the metal propellant that is used [Ref. 6]. The typical spot lasts for <1 µs: hence, during a typical 5ms duration arc discharge, there are thousands of such spots that wink on and off across the puck surface. The spots are randomly distributed and over millions of pulses cover most of the available surface. Figure 6 shows a cartoon of how these individual spot plasmas expand to fill a cone of roughly ±30° half-angle.

The erosion rate of refractory metals such as Molybdenum (Mo) and Niobium (Nb) is ~35 μg/C [Ref. 6]. For an arc of 0.6 Coulomb total charge, the mass eroded is ≈20 μg/pulse. At a speed of 17.4 km/s (Mo target), the ideal impulse-bit created by each pulse is 0.31 mNs. This ideal impulse bit is reduced by three deleterious factors: the hot plasma expands into a "supersonic" cone of $\pm 30^0$ about the axis. The radial component of momentum reduces the thrust to 85% of the purely axial value; the plasma is not fully ionized. Refractory metals such as Mo are found to be doubly ionized in such arcs but nevertheless the ion fraction is only about 95%; lastly, the anode (see Figure 1) is not 100% transparent. The anode's transparency varies from shot to shot depending upon where the cathode spots are created and how they propagate across the puck during the ~5ms arc period. For a typical (averaged over the area) anode transparency of 80%, the product of these three deleterious corrections is 95% x 85% x 80% = 65%. The ideal impulse bit of 0.31 mNs is reduced to 0.2 mNs. At a pulse repetition rate of 5 Hz, the ideal thrust produced is approximately 1 mN. Erosion creates a deepening well in the puck that eventually ejects most of the available metal into space, leading to end-of-life of the puck. Each square Mo puck pair begins with a mass of 130 g. If all of the puck is eroded, it would generate ~1430 Ns of total (useful) impulse. The four pucks could give a total mission impulse up to 5.7 kNs, from a thruster volume of 96 mm x 96 mm x 68 mm, or ~0.6 U.

III. EVOLUTION OF MPT THRUSTERS OVER TIME

Four NASA SBIR awards [Refs. 7 - 10] have enabled AASC to mature the technology in 5 years from a TRL4 lab-scale prototype to a TRL7, flight worthy product. Figure 7 shows the evolution of the MPT, via various design iterations.

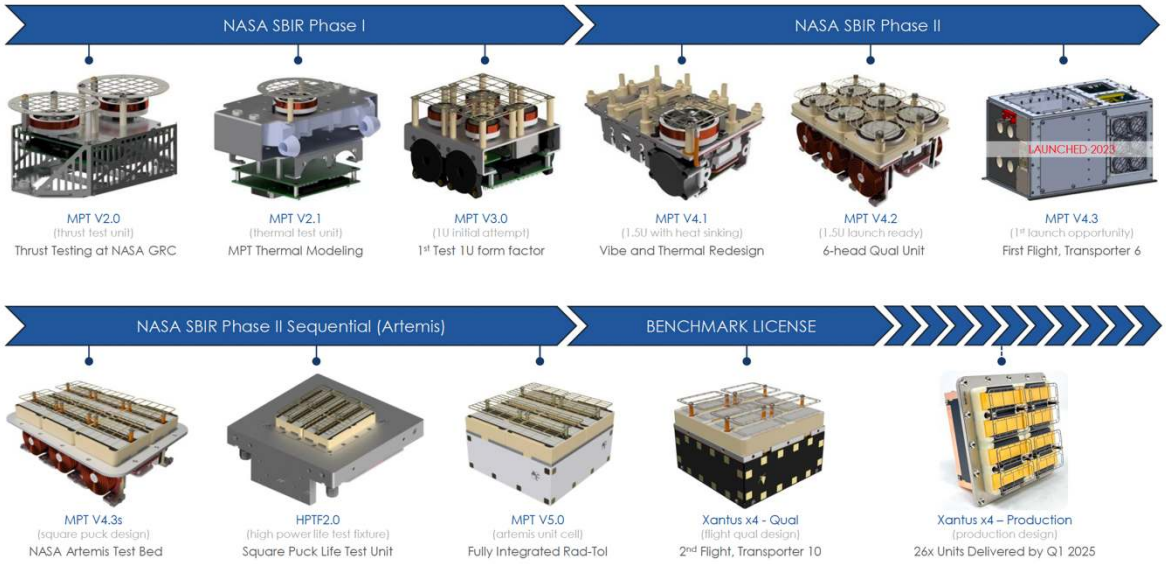


Figure 7: NASA SBIR contract funded evolution of MPT from 2018 -2024

While the early work centered around proving that the technology was feasible as a thruster module (MPT2.0, 2.1 and 2.3), the later projects aimed to prove that the technology could become a design qualified to fly and operate in space (MPT4.1, 4.2 and 4.3), culminating in delivery of a flight-worthy unit to Orion Space Systems/Colorado, for integration into their 18 kg satellite built for the USSF RROCI (Rapid Revisit Optical Cloud Imager) mission.

This flight-worthy prototype was launched into LEO in January 2023, but the deployer failed and it burned up on reentry. A second unit was integrated into the same type of satellite and launched into LEO on March 04, 2024. This time the satellite was successfully deployed into LEO. A third launch with four MPT thrusters (dubbed Xantus and built by licensee Benchmark Space Systems) is planned to launch on another Orion Space (now Arcfield) Satellite in August 2025. We have conducted extensive firings in

vacuum on the ground (>15000 hours) and have measured thrust and impulse at NASA in the GRC/VF-3 facility and have published the results [Refs. 2 & 12].

Currently we build (at licensee Benchmark's facility) in batches of ~6x units as that is the number of units that can fit in both the production puck conditioning chamber as well as the TVAC chamber (Figure 8) and build on a 3 week cadence, where the first week is unit assembly, the second week is conditioning + vibe, and the third week is TVAC + final run. Thirty such units have been assembled, qualified and will be shipped to different customers (by licensee Benchmark) before June 30, 2025.



Figure 8: Six Xantus units installed in TVAC chamber at Benchmark

IV. IMPULSE AND THRUST MEASUREMENTS AND THEORETICAL ESTIMATES

The Torsional Thrust Stand (Figure 9) was housed in the VF-3 test facility at NASA/GRC. The vacuum chamber is 1.5 m in diameter and 4.5 m long and is evacuated by either four oil diffusion pumps (ODPs) or one turbomolecular pump, backed by a roughing pump. The pumping speed of the ODPs is 80,000 liter/sec at 0.05 mPa. Facility pressure was measured with two Granville-Phillips micro ion gauges, both located on the facility wall. One gauge was within 1 meter of the thruster and the other was located at the opposite end of the facility; both gauges were monitored and recorded during testing. Typical background pressure during MPT testing was 0.1 mPa.



Figure 9: VF-3 facility at NASA/GRC



Figure 10: MPT5.0-005 Mounted on thrust stand in VF-3

Figure 10 shows the Xantus unit mounted on the torsional thrust stand. This thrust stand was used to measure impulse bits from the pulsed MPT. A review of the development and operation of the thrust stand

can be found in the work by Haag [Ref. 7]. The working principle of the pendulum thrust stand is that each firing of the MPT causes a deflection of the pendulum that subsequently rings down like a harmonic oscillator.

The thrust stand was used to determine impulse bit as a function of thrust stand deflection, spring stiffness, and natural frequency. In-situ calibration weights were used to apply a known static force to determine the static deflection of the thrust stand. Thrust stand deflection was measured using a linear-variable differential transformer (LVDT) and natural frequency was measured by allowing the stand to oscillate under a nearly un-damped condition.

The thrust stand was equipped with a damping actuator capable of operating in a near un-damped state or a near critically damped state. The actuator was enabled or disabled external to the facility to allow measurement of calibration weights, natural frequency oscillations, or thruster impulse bits as needed. The stand was also equipped with a two-axis inclinometer and set of piezoelectric actuators to ensure consistent inclination of the thrust stand during calibration and thruster measurement. The measurement uncertainty in the impulse-bit was estimated to be ±2%.

A. Mo targets

This section presents summary results from several test campaigns carried out at the VF-3 vacuum facility at NASA/GRC. These results have been published in earlier papers. Here we present a condensed summary, to motivate a comparison of the MPT with its peers in the next section of this paper.

Table 1 shows how the impulse bit is calculated for a single shot from Puck 1. There are four Mo pucks (see Figure 1), but the calculations are shown only for Puck 1 (on top left of the figure).

TABLE 1: Calculated and measured Impulse bits: Mo puck #1 at 45V charge

Puck	V_initial, V	V_final, V	Charge into arc, C	calculated impulse bit, mNs	measured impulse bit, mNs	Anode Transmission
1	45	28.7	0.359	0.218	0.160	91%

Table 1: Measured and estimated impulse bits: first campaign.

The initial charge voltage on the primary capacitor (see 206 in Figure 3), V_initial, is 45 V. After the discharge of ~3 ms duration, the voltage has dropped to V_final of 28.7 V on this shot (column 3 of Table 1). The voltage difference and the smaller capacitance of this unit give the charge into the arc as 0.359 C (column 4). In section **I** we quoted a charge of 0.6 C, but that was using a larger capacitor in the PPU. For these tests we used a smaller capacitor. This *measured charge suffices* to estimate the ideal impulse bit (I-bit), given as:

*I-bit=charge into arc (0.359 C) * erosion rate for Mo (35 μg/C) * ion speed (17409 m/s) = 0.218 mNs.*

How did we assign the erosion rate and plasma speed for these arcs? The textbook by Anders [Ref. 6] contains comprehensive data on cathodic arcs that have been studied for several decades. Key parameters such as erosion rate, ion speed and degree of ionization have been measured or estimated for dozens of metal elements. Table 2 shows relevant data for Mo, Cu and Fe (as a substitute for stainless steel) that have been culled from Anders. The values reported by Anders were measured under arc conditions (peak current and pulse width) that *are very similar to those* in our MPT.

The Cohesive Energy Rule for vacuum arcs postulated by Anders describes an empirical relationship between the cathode material and the arc burning voltage, namely, that the burning voltage (column 3) depends approximately linearly on the cohesive energy (column 2). The ion kinetic energy (column 4) gives the ion speed (column 5). Anders and several others have made detailed measurements of the ionization fraction and erosion rates in cathodic arcs. The currents and pulse durations of these measurements are very similar to those of the Xantus thruster, so we will assume the values given in Table 2.

cathode material	cohesive energy (eV/atom)	arc burning voltage (V)	ion kinetic energy (eV)	Ion speed, m/s	Ionization Fraction, %	Erosion rate, µg/C
Fe	4.28	22.7	46	12677	78%	32
Cu	3.49	23.4	57	13229	72%	35
Mo	6.82	29.3	149	17408	95%	35

Table 2: Key parameters for cathodic arcs of Mo, Cu and Fe

The Mo erosion rate (Table 2) is ≈35 µg/C. The product of 0.359 C charge and erosion rate gives the mass ejected from the puck surface as 12.6 µg. The measured ion speed is 17,408 m/s. Hence the (ideal) impulse bit on this shot is 0.218 mNs (column 5 of Table 1). The metal plasma thruster is unique among all electric propulsion thrusters in that its impulse (thrust) may be estimated so easily using a single measured electrical parameter. This ideal impulse bit must be corrected for real-world inefficiencies as mentioned earlier. We fix the ionization fraction and plume divergence at 95% and 85% respectively, as before. The ionization fraction is from Anders [Ref. 6]. The plume divergence correction is a complex convolution of radial plasma flux profile and radial ion velocity profile, integrated over the solid angle. For now, we simply assume it is 85%. This leaves the (variable) anode transmission as a free parameter, that is calculated to be 91% for this shot (see Table 1).

	V_initial, V	V_final, V	measured impulse bit, mNs	Energy into arc, J	Thrust energy, J	Thrust Efficiency, %	Thrust/Power, mN/kW
1	45	28.7	0.160	13.2	1.39	10.5%	12.1

Table 3: Thruster parameters with a Mo puck

Table 3 shows how we use the measured impulse bit (0.160 mNs) and speed (17408 m/s) to calculate other thruster parameters. The measured final voltage of 28.7 V gives the energy delivered to the arc as 13.2 J. The thrust energy is given by the ejected mass Δm (12.6µg) and ion speed (17408 m/s) as 1.39 J. The thrust efficiency is calculated from:

$$\eta_{thrust} = \frac{\frac{1}{2} I_{bit} u}{\Delta E} \quad = \frac{\frac{1}{2}\Delta m\, u^2}{\frac{1}{2} C \left(V_i^2 - V_f^2\right)} \tag{1}$$

Rewritten as:

$$\eta_{thrust} = \frac{0.5 * \Delta m * u^2}{0.5 * C * (V_i^2 - V_f^2)} = \frac{0.5 * \varepsilon * C(V_i - V_f) * u^2}{0.5 * C * (V_i^2 - V_f^2)} = \frac{\varepsilon * u^2}{(V_i + V_f)} \tag{3}$$

where V_i is the initial charge voltage of the PPU capacitors, V_f the burning voltage of the arc (at which the arc current cuts off), I_{bit} is the measured impulse bit and C is the capacitance. ΔE is the energy dissipated by the thruster/pulse, calculated from the measured voltage on the capacitor at the start and at the end of the pulse. This method of estimating the efficiency considers all the losses in the driver circuit as well as the thruster inefficiency. Hence the thrust efficiency is 10.5% for this shot and lastly, the thrust/power ratio (T/P) is calculated to be 12.1 mN/kW. This 12 mN/kW value implies that a 40 W Xantus thruster (operating on a 30kg – 50kg satellite) would provide a thrust of ≈0.5 mN. In VLEO for example, this thrust would combat atmospheric drag for such a satellite making excursions from 300 km down to 200 km in elliptical orbits (to sample the ionosphere or take optical and infrared images) for 115 days, assuming a total impulse of 5 kNs.

SHOT #	Impulse bit (measured)	Impulse bit (ideal)	Impulse bit correction factor	Thrust efficiency	Thrust/Power
Mo	mNs	mNs	measured/ideal	%	mN/kW
1	0.422	0.708	0.60	9.9%	11.40
2	0.353	0.657	0.54	8.8%	10.08
3	0.364	0.637	0.57	9.3%	10.64
4	0.365	0.637	0.57	9.3%	10.65
5	0.444	0.677	0.66	10.8%	12.40
6	0.424	0.677	0.63	10.3%	11.83
7	0.428	0.708	0.61	10.1%	11.58
8	0.464	0.758	0.61	10.4%	11.95
9	0.445	0.698	0.64	10.6%	12.15
10	0.400	0.667	0.60	9.8%	11.28
11	0.457	0.738	0.62	10.4%	12.00
12	0.402	0.677	0.59	9.8%	11.22
13	0.423	0.677	0.62	10.3%	11.80
14	0.404	0.607	0.67	10.7%	12.25
15	0.375	0.738	0.51	8.6%	9.84
16	0.308	0.718	0.43	7.2%	8.24
17	0.450	0.688	0.66	10.8%	12.43
18	0.441	0.546	0.81	12.6%	14.53
19	0.441	0.667	0.66	10.8%	12.45
20	0.352	0.597	0.59	9.4%	10.82
21	0.408	0.586	0.70	11.1%	12.70
22	0.349	0.667	0.52	8.6%	9.86
23	0.359	0.708	0.51	8.5%	9.72
24	0.439	0.677	0.65	10.7%	12.26
25	0.445	0.708	0.63	10.5%	12.02
26	0.376	0.657	0.57	9.3%	10.72
27	0.459	0.672	0.68	11.2%	12.86
average	0.407	0.672	61%	10.0%	11.5
mean standard deviation (σ)	0.042	0.048	0.072	0.011	1.262
σ, %	10.3%	7.2%	11.9%	11.0%	11.0%

Table 4: Calculated and measured impulse bits: Mo pucks at 45V charge.

With this background, Table 4 presents data from 27 shots during an early thrust measurement campaign at NASA/GRC in the VF-3 Thrust stand facility. Column 1 shows shot numbers. Column 2 shows the measured impulse bits using the thrust stand. Column 3 shows the calculated ideal impulse bit, using only the eroded mass (from the charge and erosion rate (see Table 2) while assuming no impulse loss due to beam divergence, 100% ionization and 100% anode transmission. Column 4 is the ratio of measured/ideal impulse bit. This is less than unity due to three deleterious correction factors: the anode transmission is roughly 85%, the ionization fraction is roughly 90%, and there is about 20% beam divergence loss due to the radial component of thrust. The product of these three terms: 85%*90%*80%= 61%, which is what is given in column 4 of the table. Earlier we estimated an anode transmission of 91%, so why are we using 85% here? Because the anode is not uniform in transmission. The cathode spots on any given shot are randomly distributed across the puck face so the anode transmission varies from a low of ≈70% in certain places up to 100% on shots where the spots happen to be located directly below the open area of the anode. Hence, we use an average transmission of 85% here. Column 5 shows the calculated thrust efficiency (11%) using the measured impulse bits and column 6 shows the calculated thrust/power ratio (11% also). These values are similar to the values shown in Table 3).

At the bottom of the table, we present average values with mean standard deviations of these parameters. The coefficient of variation of the measured I_{bit} (10.3%) is higher than the calculated (7.2%) coefficient of variation. This is because the impulse bits are emitted at randomly distributed locations across the 38mm diameter target face of this unit. Hence the lever arm from these locations to the fulcrum of the torsional

stand varies by up to 19 mm off center. Since the thrust stand calibration assumes that the thrust is always emitted from the center of the target, this introduces an artificial error in the measured impulse if the arcs were not symmetrically disposed about the target centroid, which is why the standard deviation variation is apparently higher.

B. Nb targets

Table 5 shows similar data taken from a Nb target at a PPU charge voltage of 35V (20J/pulse into the arc). This test ran a sequence of 30 shots with a Nb target. Column 4 shows that the ratio of measured/ideal I_{bit} is 57%. From this the ionization fraction F may be calculated as: F=0.57/(0.9x0.85) = 75%. Nb, as is Mo, is a refractory metal. The literature [Ref. 6] reports ionization fraction ~80%-85% for Nb. Here we ran the target at a relatively low current (only 35V PPU charge), so the ionization fraction is lower. Hence the Nb ion fraction of 75% at the lower charge voltage of 35V is consistent with this trend. The shot-shot spread with Nb is higher than with Mo but may be reduced by accumulation of a larger number of shots in a given run.

SHOT #	Impulse bit (measured)	Impulse bit (ideal)	Impulse bit correction factor	Thrust efficiency	Thrust/Power
Nb target	mNs	mNs	measured/ideal	%	mN/kW
1	0.165	0.331	0.50	7.0%	8.53
2	0.182	0.322	0.56	7.9%	9.66
3	0.195	0.322	0.60	8.5%	10.34
4	0.179	0.322	0.55	7.8%	9.48
5	0.186	0.322	0.58	8.1%	9.90
6	0.222	0.396	0.56	8.1%	9.83
7	0.196	0.341	0.58	8.1%	9.91
8	0.188	0.322	0.58	8.2%	9.97
9	0.173	0.304	0.57	7.9%	9.68
10	0.214	0.368	0.58	8.3%	10.09
11	0.185	0.331	0.56	7.8%	9.57
12	0.237	0.414	0.57	8.3%	10.08
13	0.187	0.350	0.53	7.6%	9.23
14	0.177	0.313	0.56	7.9%	9.62
15	0.208	0.359	0.58	8.2%	10.04
16	0.163	0.295	0.55	7.7%	9.37
17	0.164	0.295	0.56	7.7%	9.43
18	0.234	0.405	0.58	8.3%	10.17
19	0.192	0.350	0.55	7.8%	9.47
20	0.190	0.341	0.56	7.9%	9.60
21	0.197	0.341	0.58	8.2%	9.95
22	0.211	0.354	0.60	8.5%	10.31
23	0.204	0.345	0.59	8.3%	10.16
24	0.181	0.313	0.58	8.1%	9.88
25	0.155	0.285	0.54	7.5%	9.18
26	0.196	0.341	0.58	8.1%	9.90
27	0.197	0.341	0.58	8.2%	9.98
28	0.179	0.304	0.59	8.2%	10.04
29	0.221	0.378	0.58	8.3%	10.18
30	0.193	0.350	0.55	7.8%	9.53
average	0.192	0.339	57%	8.0%	9.8
mean standard deviation (σ)	0.020	0.032	0.021	0.003	0.390
σ, %	10.50%	9.31%	3.69%	3.99%	3.99%

Table 5: Measured and estimated impulse bits: Nb target at 35V charge

C. Reproducibility of Nb target

To gauge the reproducibility of the impulse, I_{bits} from a Nb target were measured for groups of 30 shots each, but with intervals between tests during which the target was allowed to run at 0.5Hz for long periods, as noted in

Nb Impulse bits measured after several long runs	
TEST PROTOCOL	Impulse bit (measured) mNs
test 1: 30 shots	0.192
test 2: 500 shots at 0.5Hz, then 30 shots	0.198
test 3: 2100 shots at 0.5Hz, then 30 shots	0.191
test 4: 4000 shots at 0.5Hz, then 30 shots	0.188

Table 6. Over such a 6720-shot sequence, the average I_{bit} measured (for 30 shots each) showed less than ±2% variation. Thrust and impulse were also measured from Cu, stainless steel and Pd targets. These have been reported elsewhere [Ref. 12] and will not be repeated here. The Cu and stainless steel data were spoiled by a contamination issue that caused the cathode spots to hover in less transparent anode regions. The MPT has been operated with a variety of metals: C, Al, stainless steel, Cu, Pd, Nb and Mo. The thrust/power ratio for many of these metals fell into the range of 8 mN/kW – 15 mN/kW.

Table 6: Impulse bits from Nb targets over long runs

D. Thrust Measurements

In addition to impulse bit measurements, a short test was conducted to directly measure thrust. For this, the MPT was operated at a higher repetition rate so that the torsional thrust stand gave a steady deflection while the thrust was applied, rather than a harmonic oscillation in response to a short impulse bit. The MPT was operated with a Pd target at three different repetition rates: 3, 5 and 10Hz. The natural resonant frequency of the trust stand is about 4Hz, so this frequency was avoided.

Freq.	Thrust	ΔE/pulse (Pd)	Power	Thrust/Power
Hz	μN	J	W	mN/kW
3.3	428	8.15	26.9	15.9
5	635	8.15	40.8	15.6
10	1270	10.3	103.0	12.3

Table 7: Thrust measurements: Pd target

Table 7 shows the measured thrust using this technique. The impulse bit measurements used up to 75J/pulse energy, but for the thrust measurements, the PPU charge voltage was reduced to 23V in order to keep the energy/pulse around 10J and hence the power relatively low. In addition, the thrust measurement was taken within seconds of operating the MPT in order to minimize heating of the MPT and the torsional thrust stand to avoid temperature changes in the stand that would change the calibration. These measurements were not as extensive as the impulse bit measurements. Nevertheless, the thrust/power derived from these measurements of ~15mN/kW compares favorably with the values deduced from impulse bit data (not shown for Pd in this paper but see Ref. 2). The lower thrust/power ratio at 10Hz is an artifact due to the limited current of the DC charging supply used to charge the PPU capacitors on this unit. The supply could not charge the capacitors back to 23V between shots and hence the actual power was lower than the 103W estimated assuming the full 10.3 J/pulse input.

E. Adaptive Firing Mode

The pulsed MPT shows large variations in impulse-bit from shot to shot. ***But this is not to be viewed as a limitation of the thruster!*** A mitigating factor is that the impulse-bit on each shot is so low (~0.2 mNs) that hundreds if not thousands of pulses are required to impart any significant Delta Vee to the spacecraft.

Table 6 shows that the impulse bit is reproducible to ±2% from one 30-pulse run to another. To put it differently, the total impulse from 30 pulses (6 mNs) varies by less than 2% from run to run. Suppose that the spacecraft mass is 60 kg? Such an impulse bit of 6 mNs imparts a ΔV of 0.1 mm/s to the craft, and this is reproducible to 2%, or 2 μm/s! The MPT enables precise and reproducible control of the attitude and position of a spacecraft.

The shot-shot variation in impulse bit is not per se a limitation for the reasons given above. But there is a technique by which we *reduced this variation even further*, by implementing an "adaptive firing rate" mode. While there is rather tight control on the energy available for each shot of the MPT (capacitor charged to +45V), the amount of energy that any given shot uses varies quite a bit. While a burned-in MPT will consistently bring the capacitor charge down towards +30V, any given shot can vary anywhere in the range of the max cap charge (+45V) voltage down to that +30V value. And while when averaged over thousands of shots the total impulse is quite reproducible, the total power going into the unit can vary significantly depending on from what post-arc voltage the capacitor needs to be recharged.

This behavior is better illustrated below in Figure 11 that shows a simplified example of two heads firing in alternation, where Head 1 consistently drains the capacitor from +45V down to +30V while Head 2 is only draining down to +35V. The MPT currently functions in one of two modes, the first being "constant firing rate" mode, meaning an arc is triggered every X milliseconds, in this case every 1000 milliseconds. For this example, this means that Head 1 is operating at about 24.8W and Head 2 at 17.6W for an average of 21.2W.

This variable power could be less than desirable for a few reasons. Firstly, it creates a bit of a trial-and-error operation for the spacecraft where the controller must try different rates to figure out a power budget to operate the MPT. Secondly, as the MPT burns through its fuel the physical length of the arc grows and the total plasma resistance can also increase, meaning a constant rate that previously operated at a certain average power/impulse would then change. Thirdly, there does seem to be a variation in performance from head-to-head which means there could be further differences depending on the shot pattern.

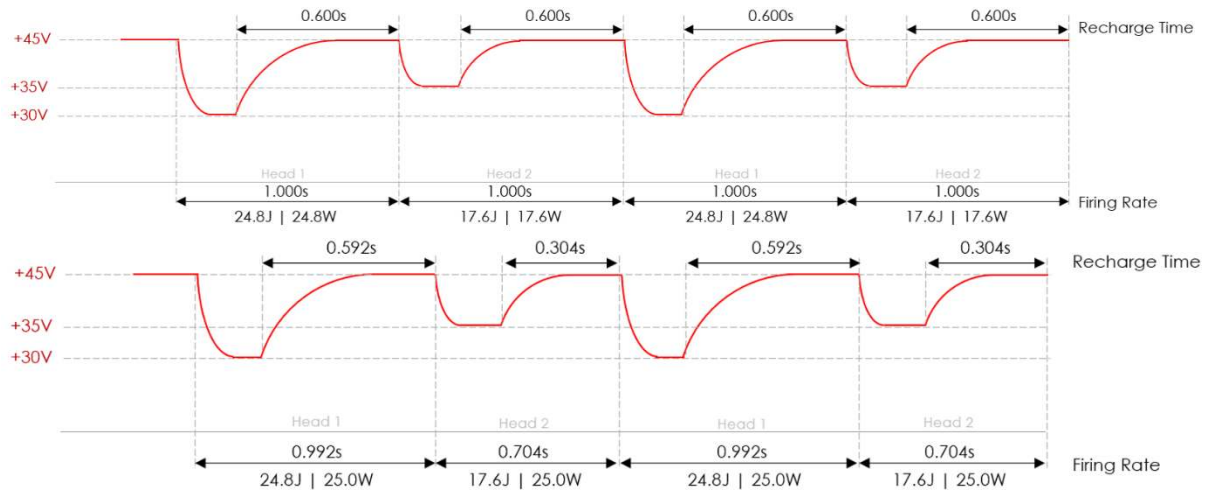


Figure 11: Constant Firing Rate mode (top) Versus Adaptive Firing Rate mode (bottom)

To improve upon this challenge, we implemented closed loop control, allowing the MPT to operate in the second mode, "adaptive firing rate" mode which adjusts the rate of firing on the fly depending on the desired output power which is set by the spacecraft. The method relies on our onboard post-shot capacitor voltage measurement. Instead of simply printing it out for telemetry tracking, the MPT uses this capacitor voltage reading to evaluate the total charge (and hence impulse) of the last shot and adjusts the next shot's timing accordingly. By implementing an adaptive recharge rate (akin to an adaptive firing rate) and a set desired power of 25W (for example), the MPT would be able to quickly sense the previous shot's total charge and then adjust the recharge time to ensure each shot lands on 25W average. Figure 11 shows a simplified example of how this works, with the same simulated performance between Head 1 and Head 2 as mentioned above. However, in this case the onboard controller adapts the timing of the following shot to achieve a constant power output of 25W.



Figure 12: Adaptive Firing Rate mode test data

Figure 12 shows a plot of the data output for a first test of the adaptive firing mode algorithm. The red scatter plot shows the shot-to-shot power when firing in constant rate mode @ 1000ms. It is worth noting that the performance for this unit is rather consistent already and hence the initial scatter is rather tight, +/- about 8W. The blue and green scatter points show closed loop control with targets of 19W and 10W respectively, which are much tighter than constant rate mode.

The tests of different pucks showed that the MPT is flexible in its choice of propellant. Any conducting metal may be used. The tradeoff is ion speed, erosion rate and puck density. Results published earlier [Ref. 12] showed that Cu and stainless steel are viable alternatives to Mo. Other tests had shown that Nb (data presented here) and Al are also viable. The versatility of the MPT has been demonstrated by operating with many types of propellant including Pd.

A simple, adaptive control algorithm enables operation at a constant power (hence a constant thrust) despite shot-shot fluctuations in impulse bits.

V. How does the MPT compare with its peers in the ~1mN class?

This section presents a comparative study of several 1 mN class EP thrusters. We consider two groups of thrusters. The first group includes the MPT, an Indium FEEP [Ref. 3] and an Iodine ion engine [Ref. 4].

Figure 13 shows images (from various websites) of the thrusters. We have selected these thrusters in the 100 W class for an apples-apples comparison.



Figure 13: ~1 mN EP systems. left: AASC MPT; middle: Enpulsion In FEEP; right: ThrustMe NPT30-12 Ion engine

The second group (Figure 14) compares the Busek BHT-350 350 W Hall thruster with the AASC MPT "Artemis Array" built for the Artemis program, as a 4x4 array of MPT unit cells (the unit cell is shown in Figure 1), that is designed for operation at up to 400 W.



Figure 14: Busek BHT-350 HET (left) shown without the PPU or Xe tank, and MPT "Artemis" array (right), built for Artemis missions: (4mN/20 kNs for 12U CubeSats in Lunar orbit)

Table 8 provides information on key parameters of the three thrusters in Figure 13.

	Thrust, mN	Power, W	Wet mass, kg	Volume, L	Total Impulse,kNs
MPT	1	100	1.4	0.60	5.7 [a]
Enpulsion FEEP MACRO r3	1	100	3.9	2.23	25.5 [b]
ThrustMe Iodine ion	1.1	75	1.2	1.0	4 [c]

[a] maximum possible impulse for total loaded Mo mass of 520 g
[b] at ISP of 2000s,consistent with 1 mN thrust for alpha emitter
[c] at ISP of 2000s, consistent with 11. mN thrust using Iodine

Table 8: Comparison of the AASC MPT with the Enpulsion FEEP and the ThrustMe Iodine ion engine

The MPT operates with Mo propellant at a fixed ISP of 1774 s. The FEEP and Iodine ion engine offer variable ISP. The thrust of the MPT is fixed at 10 μN/W (as discussed earlier) but the thrust of the other two devices varies as ISP is varied. To compare with the MPT, we have chosen fixed operating points at 2000 s ISP for these thrusters, at which their thrust (column 1) is comparable to that of the MPT. The Iodine ion engine operates at lower power (column 2) and hence gives a higher thrust/power ratio that the other two. However, the MPT has the lowest volume (column 4) with a wet mass comparable to that of the Iodine ion engine. The FEEP has a higher wet mass. These masses include the PPU in all cases. Lastly, we examine the total impulse from these engines. The MPT and Iodine ion engine offer comparable total impulse (4 kNs – 5.7 kNs when propellant is fully exhausted), but the FEEP claims an impulse as high as 25.5 kNs. This is consistent with its higher wet mass and volume.

The satellite designer would take the mission CONOPS into consideration when choosing amongst these candidates. Where mass and volume are a priority, the MPT wins. Where total impulse (mission Delta Vee) is more important, the FEEP offers higher impulse.

The AASC MPT is notable for its simplicity of design, rugged, low voltage PPU, cold start after long dormancy (for end of life deorbit), low mass and volume.

Table 9 provides information on key parameters of the two higher power thrusters in Figure 14.

	Thrust, mN	Power, W	Wet mass, kg	Volume, L	Total Impulse,kNs
MPT "Artemis" Array	4	400	5.6	2.40	22.8 [a]
Busek BHT-350 Hall Thruster	17	350	9.7	≈6	75 [b]

[a] maximum possible impulse for total loaded Mo mass of 2080 g

[b] at ISP of 1244s, quoted for the 17 mN nominal thrust at 350 W

Table 9: Key parameters of the Busek350 Hall Thruster and the MPT "Artemis" array

The Hall Effect Thruster (HET) stands out for its nearly five times much higher Thrust/Power (T/P) ratio, which implies a higher thrust efficiency. Because the propellant is stored separately from the thruster head and PPU, the Hall Thruster inherently takes up more volume in a spacecraft. The estimates of wet mass and volume for the HET in Table 9 were made by assuming Xe propellant stored at 1.6 g/cc, an estimated Xe tank volume/mass, and adding the published masss of the PPU and thrusuer head. The trade between these choices will depend upon the mission constraints. Where wet mass and volume are a priority, the MPT always wins. If a satellite designer chooses to install an HET that is rated only for 23 kNs (same as the MPT "Artemis" array), even then the HET wet mass and volume would be higher than those of the MPT array, due to the lower ISP of the HET (more propellant required) and the lower density of liquid Xe (1.6 g/cc) versus that of the solid Mo (10.22 g/cc). The MPT propellant density is 6x that of high pressure Xe in Hall thrusters (HETs) and 2x that of Iodine. The MPT works with a variety of metals and alloys. Measurements have been made with C, Al, Cu, steel, Nb, Pd and Mo.

The MPT can also operate with Platinum whose density of 21.5 g/cc is ≈5x higher than that of Iodine and 14x higher than that of Xe in HETs. For deep space missions, such an advantage allows a larger propellant budget within a smaller spacecraft volume.

Another observation when comparing the HETs with the MPT is that the Hall thrusters do not scale well to powers <100 W. Busek has a BHT-100 device on offer but going below 100 W is not easy for a Hall thruster. The MPT on the other hand, operates reliably at any power (even as low as 1 W) while giving the same fixed thrust/power ratio of 10 μN/W. This is an important considreation. The FEEP, Iodine ion engine and HETs all require standby power for heaters or electron neutralizers. Hence they cannot operate at very low powers (<10 W). For certain mission phases and for smaller spacecraft that are power limited, this is a dinstinct advantage of the MPT.

DISCUSSION OF KEY OPERATING PARAMETERS

What are the key parameters of any thruster for the mission planner?

- Thrust (a key CONOPS parameter for duration of maneuvers)
- Thrust efficiency, related to T/P ratio (key for thermal management/soak back)
- Total impulse (key parameter to determine total Delta Vee possible)
- Impulse/mass (determines available payload mass)
- Impulse/volume (determines available payload volume)

All but the Hall thruster offer ~1 mN thrust, whereas the Hall is rated at 17 mN. The higher thrust enables faster maneuvers. For example, a collision avoidance maneuver would take 17x shorter time. But even 17 mN thrust is not high enough for rapid collision avoidance if the satellite mass is high.

Let us look at an example: Suppose that a 50 kg nanosatellite is warned of an imminent conjunction and must move by 5 km to avoid it. The Delta-vee required from a 400 km orbit is ≈2.8 m/s. A 1 mN thrust applied to the satellite would take almost 40 hours to move the satellite down to a 395 km orbit. The Hall thruster at the same power would require only 2.4 hours. If the conjunction is predicted by NORAD or by an on-board software package that tracks possible interfering satellites and there is adequate advance warning of the possibility, a 40 hour maneuver might suffice. The problem is the unexpected conjunction: for example, a debris object from a shattered object that is not being actively tracked and gives warning of imminent danger only an hour or two in advance. In such a case, The HET or a chemical propulsion kit is a safer bet. Even 100 mN of thrust would reduce the time for the evasive maneuver from 40 hours to 24 minutes.

One prudent mission choice might be to combine EP with a less efficient Chem. Prop. (CP) solution that is used primarily for collision avoidance and rapid orbital changes such as phasing into a desired orbit after launch, to begin revenue generating operations quickly. The far more efficient EP would be used for slower mission CONOPS such as fine pointing, momentum wheel desaturation or other maneuvers. If a Hybrid CP/EP system is chosen, the combined mass and volume would be lower than for a CP solution alone, for the same total Delta Vee.

A more prudent choice might also be to combine a Hall Thruster with the MPT. Then the mission planner has at her disposal a choice of higher thrust (~10 mN- 20 mN) for the HET for mission phases that require rapid maneuvers with the lower thrust (~1 mN) of the MPT being used efficiently for those maneuvers that can accept a slower action duration. Examples of such choices would be rapid phasing after launch into desired (revenue generating) orbits done using HET or fine positioning or small orbit transfers that could be done using MPT. Another mission CONOPS that will become increasingly important is RPOD (Rendezvous, Proximity Operations and Docking) maneuvers. Given the high value of the target satellite (for refueling or other maintenance) and the complexity of the docking maneuver (consider a tumbling target), the HET could be used to approach the target, but for the last 10% of the distance between targets, the pulsed, lower thrust MPT would be used to close the gap with high precision.

The attributes considered above are numeric and allow quantitative comparison. But there are non-quantitative attributes that are also important.

One such is the PPU voltage. The FEEP and Iodine ion engine require high voltage (>1 keV) for operation. This poses a challenge when gaps are small (such as between grids). The In FEEP has a long history of operation in space. There are published instances of grids shorting due to liquid droplet buildup when the engine is operated at the higher end of its thrust envelope. None of these thrusters operates with plasma at 100% ionization efficiency. The refractory Mo used in the MPT has been shown [Ref. 6] to have 95% ionization. Yet the 5% that is neutral vapor or atoms is not ejected normal to the target (cathode) at high velocity, but is an effusive ejection. Hence there is always some build-up of Mo atoms on thruster surfaces that could lead to electrical shorts and end-of-life. Extensive tests in vacuum (>15,000 total hours of operation) have uncovered such premature shorting and steps were taken to mitigate/eliminate it. With more extensive vacuum testing, the MPT could realize its full potential total impulse of 5.7 kNs from a 0.6 L volume. The low DC voltage of only 45 V in the MPT PPU makes it more reliable than the higher voltage boards in the other thrusters. High voltage in tight spaces is a challenge to avoid dielectric breakdown. If the gaps are increased to mitigate this, then the overall volume becomes larger.

Another attribute is ruggedness: The MPT does not require special handling (booties, gloves, masks) during assembly and qualification or during spacecraft integration. Once the pucks (Mo or other metals) are conditioned (in vacuum requiring <50,000 shots at 25 W, which takes 14 hours at 1 Hz rep-rate), they may be exposed to air and fire at full thrust immediately upon testing in vacuum. The FEEPs require more sophisticated fabrication of the W needles that convey the molten Indium to the emitter tips. The Iodine engine requires careful handling of Iodine in air as it is corrosive. The Hall thruster requires careful handling

of the electron gun neutralizer if it has exotic inserts. The simplicity of the MPT structure is an advantage in this regard.

A third intangible advantage of the MPT is that it may be almost fully tested in air! All of the other thrusters must be in vacuum to be tested. But the MPT trigger may be tested in air. How does this work? The MPT trigger is a plasma discharge across a conducting thin film on the periphery of the pucks. When the PPU is fired in air, these sparks are audible and visible to the naked eye, confirming that the pulsed trigger voltage is being applied to all the pucks in the array. When inside the vacuum (or in space), this trigger will initiate an arc between the puck and the anode. The MPT may thus be tested (after integration with the satellite and even just before integration with the launcher) while the others cannot be confirmed as operational until after deployment in space.

VI. Summary

Section VII has looked at several EP systems in the 100 W category and provided a rational basis for direct comparison. While no single thruster stands out well above its peers, certain advantages of the MPT are pointed out, some quantitative and others qualitative, but important for source selection by a mission planner.

VII. CONCLUSIONS

This paper has presented measurements of impulse bits and thrust from a metal plasma thruster, dubbed the MPT. Xantus has no moving parts, no liquids or gases or valves and uses a relatively simple 45V PPU. The tests described here demonstrate that Xantus may be operated with any conducting metal across the periodic table, which gives the mission planner options. Operation with Molybdenum pucks show thrust/power ratio of around 10 mN/kW up to 12 mN/kW. This is a ~1mN class thruster for microsatellites with mass in the 50 kg – 150 kg range. The basic unit cell thruster measures 96mm x 96 mm x 68 mm or a volume of ~0.6 U. The four pucks in such a volume with a total mass of 520 g can give a maximum impulse of 5.7 kNs. The thruster is scalable. Life tests continue towards a demonstration of 5 kNs or higher from the unit cell. For NASA's Artemis mission, we have configured four such unit cells as a 4.8 kg/2 U package that should give a total of 22 kNs. That impulse would be adequate to drive a cis-lunar trajectory and maintain a 12 U or 16 U satellite in lunar orbit for many months. Larger satellites would use larger arrays. The limitation is thermal management. The thrust efficiency of the Xantus is only ~10%. Even accounting for radiative emission from the hot plasma plume, up to 75% - 80% of the input power has to be conducted from the thruster and radiated into space from the satellite structure. One version of Xantus has been launched into LEO on March 4, 2024. A third launch and operation in VLEO is planned for August 2025.

VIII. ACKNOWLEDGMENTS

The authors would like to thank NASA's Small Satellite Technology Program, NASA John H. Glenn Research Center, for providing facility support, project support, and funding the facility tests at NASA/GRC. Funding for Krishnan and Frankovich was made possible by NASA space act agreement NASA SAA3-1566 and NASA Small Business Innovative Research Contracts [Refs. 8 – 11]. There are no conflicts of interests or competing interests. All authors whose names appear on the submission made substantial contributions to the conception or design of the work; the acquisition, analysis, or interpretation of data; drafted the work or revised it critically for important intellectual content; approved the version to be published; and agree to be accountable for all aspects of the work in ensuring that questions related to the accuracy or integrity of any part of the work are appropriately investigated and resolved.

IX. REFERENCES

1. Krishnan, M., Velas, K., and Leemans, S., "Metal Plasma Thruster for Small Satellites, " AIAA Journal, Vol. 36, No. 4, 2020, pp. 535-539
2. Mahadevan Krishnan, Kent Frankovich and Jonathan A. Mackey, Journal of Propulsion and Power: Impulse Bit Measurements from Metal Plasma Thruster, https://doi.org/10.2514/1.B38191
3. www.enpulsion.com
4. www.thrustme.fr
5. www.busek.com
6. Anders, A., Cathodic Arcs: From Fractal Spots to Energetic Condensation, Springer Series on Atomic, Optical, and Plasma Physics, Springer-Verlag New York, New York, 2008
7. T.W. Haag, “Thrust stand for pulsed plasma thrusters,” Review of Scientific Instruments, vol. 68, pp. 2060–2067, 1997
8. Phase I NASA SBIR Contract 80NSSC18P2214
9. Phase II NASA SBIR contract 80NSSC19C0223
10. Phase II-S NASA SBIR contract 80NSSC21C0615
11. NASA CCRPP contract 80NSSC23CA178
12. Kent Frankovich, Mahadevan Krishnan, Jonathan A. Mackey and Hani Kamhawi, Qualification of a Pulsed, Millinewton Class Metal Plasma Thruster for Broad Mission Applications, Journal of Propulsion and Power, to be published